Cancer Imaging (2013) **13(4),** 512–519
DOI: 10.1102/1470-7330.2013.0040

ARTICLE

Quantitative characterization of hepatocellular carcinoma and metastatic liver tumor by CT perfusion

Koichi Hayano[a], Gaurav S. Desai[a], Avinash R. Kambadakone[a], Jorge M. Fuentes[a], Kenneth K. Tanabe[b], Dushyant V. Sahani[a]

[a]Division of Abdominal Imaging and Intervention, Department of Radiology, Massachusetts General Hospital, Boston, MA 02114, USA [b]Division of Surgical Oncology, Department of Surgery, Massachusetts General Hospital, Boston, MA 02114, USA

Corresponding address: Dushyant V. Sahani, Department of Radiology, Division of Abdominal Imaging and Intervention, Massachusetts General Hospital, 55 Fruit Street, White 270, Boston, MA 02114, USA.
Email: dsahani@partners.org

Date accepted for publication 29 August 2013

Abstract

Purpose: To evaluate the diagnostic value of computed tomography perfusion (CTP) in the distinction of hepatocellular carcinomas (HCCs) from metastatic liver tumors. **Materials and methods:** CTP data from 90 liver tumors (HCC 38, metastasis 52) in 31 patients (16 men and 15 women; mean age 60.3 years) were studied. CTP was performed on a 16/64 multidetector-row CT scanner using a 30-s duration cine acquisition after rapid bolus injection (5–7 ml/s) of 50–70 ml of iodinated contrast medium. The CTP data were analyzed using a deconvolution model. Metastatic tumors were grouped into hypovascular ($n = 36$) and hypervascular ($n = 16$) tumors. **Results and conclusion:** The hypovascular metastases showed a significantly lower blood flow (BF) and blood volume (BV), and higher mean transit time (MTT) than HCC (all $P < 0.0001$). BF, BV, and MTT of HCCs were substantially lower than those of hypervascular metastases ($P = 0.02$, $P < 0.0001$, $P = 0.03$, respectively). A receiver-operating characteristic analysis showed that BV was a useful marker to distinguish HCCs from hypervascular metastases.

Keywords: *Computed tomography perfusion; hepatocellular carcinoma; angiogenesis; metastatic liver tumor.*

Introduction

The incidence of primary malignancies in the liver, such as hepatocellular carcinoma (HCC), is rapidly increasing[1]. On the other hand, liver is a common site for malignant tumors, especially metastases from various primaries in the abdomen and elsewhere in the body. Moreover, benign liver lesions are also frequently encountered in patients at risk for developing malignancies. Over the last several years, imaging features on computed tomography (CT) and magnetic resonance imaging (MRI) have become accepted for characterizing certain benign lesions such as hemangiomas, focal hyperplasia and, to some extent, hepatocellular adenomas[2]. A similar trend is now being extended for the diagnosis of malignant lesions, especially HCC, using imaging findings[3].

On contrast-enhanced CT (CECT), HCC is a highly vascular tumor by virtue of neoangiogenesis, and also shows hypervascular pattern of enhancement in the arterial phase[4–6]. Most metastatic tumors in the liver appear hypovascular or lower in attenuation relative to the surrounding parenchyma[4]. On the other hand, metastases from primaries such as renal cell carcinoma, endocrine tumor, carcinoid, and melanoma often have a hypervascular appearance, with elevated attenuation in the arterial phase of CECT[4]. Thus an overlap in the enhancement pattern of HCCs and hypervascular metastases in the liver can exist despite differences in the underlying tumor biology and angiogenesis between HCC and metastases[7]. Therefore, it is sometimes difficult for dynamic CT to distinguish between HCC and hypervascular metastasis because of their similar appearance[4]. Tissue sampling for the diagnosis is considered most accurate, but invasive, and therefore impractical for longitudinal monitoring. An in vivo method to differentiate liver tumors is therefore highly desirable for diagnostic purposes and treatment planning.

CT perfusion (CTP) enables quantification of tumor vascularity by measuring the temporal changes in tissue density following intravenous contrast administration[8]. Since it was first described by Miles et al.[8], CTP has been successfully applied in a variety of clinical conditions including assessment of liver cirrhosis[9,10], characterization of liver tumors[11–13], and evaluation of therapy response in liver diseases[14,15]. Tumor perfusion measurements on CT have been found to reflect the microvascular changes of tumor angiogenesis and to correlate with tumor biology[16,17]. Therefore, we analyzed CTP measurements of HCCs and liver metastases in an effort to investigate whether the CTP parameters can separate HCCs from metastases, including hypervascular ones.

Materials and methods

Patient population

This study was in compliance with Health Insurance Portability and Accountability Act regulations, and was approved by the institutional review board. All patients were required to provide written informed consent before study participation according to institutional and federal guidelines. The patient eligibility criteria included the following: (1) patients had histopathologically proven measurable locally advanced or recurrent HCC, or histopathologically proven measurable metastatic tumors in the liver; (2) patients had undergone recent contrast-enhanced MRI (CE-MRI) examination of the liver and had follow-up CT and MRI examinations over a 6-month interval to confirm tumor growth or response; (3) patients underwent no liver surgery, chemotherapy, immunotherapy, or liver radiotherapy within 4 weeks of enrollment; (4) patients had adequate renal function (serum creatinine level <2.0 mg/dl (177 μmol/l)). Exclusion criteria included the following: (1) concurrent second malignancy; (2) significant medical comorbidities; (3) clinically significant cardiovascular disease including uncontrolled hypertension, myocardial infarction, and unstable angina; (4) pregnancy or lactation; (5) known CNS metastases; (6) an inability to give written informed consent. Twenty-three patients with HCC, who were a part of a clinical study of advanced HCC[13,16], were enrolled in this study from July 2004 to January 2005, and 10 patients with metastatic liver tumors were enrolled from June 2010 to June 2012.

Imaging studies

CTP was performed using a 16/64-section multidetector-row CT scanner (Light Speed/Discovery; GE Medical Systems, Milwaukee, WI, USA). First, CT scanning was performed without intravenous contrast medium (CM) to localize the tumor. The tumor was localized on a nonenhanced CT scan, and 4–8 adjacent 5-mm sections were selected at the level of the tumor for cine imaging. In patients with solitary hepatic tumors, the portions of the tumor with the largest volume were selected for dynamic CT evaluation. The areas with definite calcifications or necrosis/cystic areas as depicted on prior imaging studies were avoided in this study. In patients with multiple hepatic tumors, the liver sections demonstrating the largest number of lesions or the largest size of lesions were selected for dynamic CT evaluation. The dynamic study of the tumors was performed at a static table position during rapid intravenous bolus injection of 50–70 ml nonionic iodinated CM (Isovue; Bracco, Princeton, NJ, USA) (300–370 mg of iodine/ml) at a rate of 5–7 ml/s. The following parameters were used: 0.5-s gantry rotation time with an interval of 1 s, 80–100 kVp, 100–200 mA, with acquisition of 4i or 8i transverse mode (4 or 8 sections per gantry rotation) and 5 mm reconstructed slice thickness. The cine CT acquisition was started about 5–8 s after the start of CM injection, and the axial CT images were acquired for a total of 30 s during breath-holding in end expiration.

Image processing

The perfusion data were transferred to an image processing workstation (Advantage Workstation 4.2; GE Medical Systems) and then analyzed using commercially available software (CT Perfusion 3.0; GE Medical Systems), which applies a deconvolution method to model CM kinetics. This analysis was performed by a single observer (K.H., with 9 years of experience in abdomen CT interpretation and CTP software). To derive functional maps of the perfusion parameters, the arterial input curve of the CM concentration is required, and we obtained this arterial input curve from a region of interest (ROI) in the aorta. ROIs for tumors were drawn freehand (using an electronic cursor and mouse) around the peripheral boundary of the visible tumor. The size range of ROIs was 14–4058 mm^2 (mean, 504.9 mm^2). Care was taken to avoid including any area outside the tumor, necrosis, or visible vessel in the ROI, which was facilitated by viewing a cine-loop of acquisition in order to gauge the degree of patient movement and the tumor margins (Fig. 1). The perfusion parameters generated by the software included blood flow (BF; in ml/100 g of wet tissue per minute), blood volume (BV; in ml/100 g of wet tissue), and mean transit time (MTT; in seconds). The CT perfusion parameters of the tumors were then calculated by averaging the functional parameters across multiple sections.

Reference standard

Liver biopsy (core and fine-needle aspiration) and histopathologic confirmation for one of the index lesions was available in all 31 patients. For the remaining 59 lesions without histopathologic confirmation, a recently performed gadolinium-enhanced MRI of the liver (performed within 2 weeks of CTP study) served as the reference standard. The additional lesions demonstrated signal intensity and enhancement characteristics identical

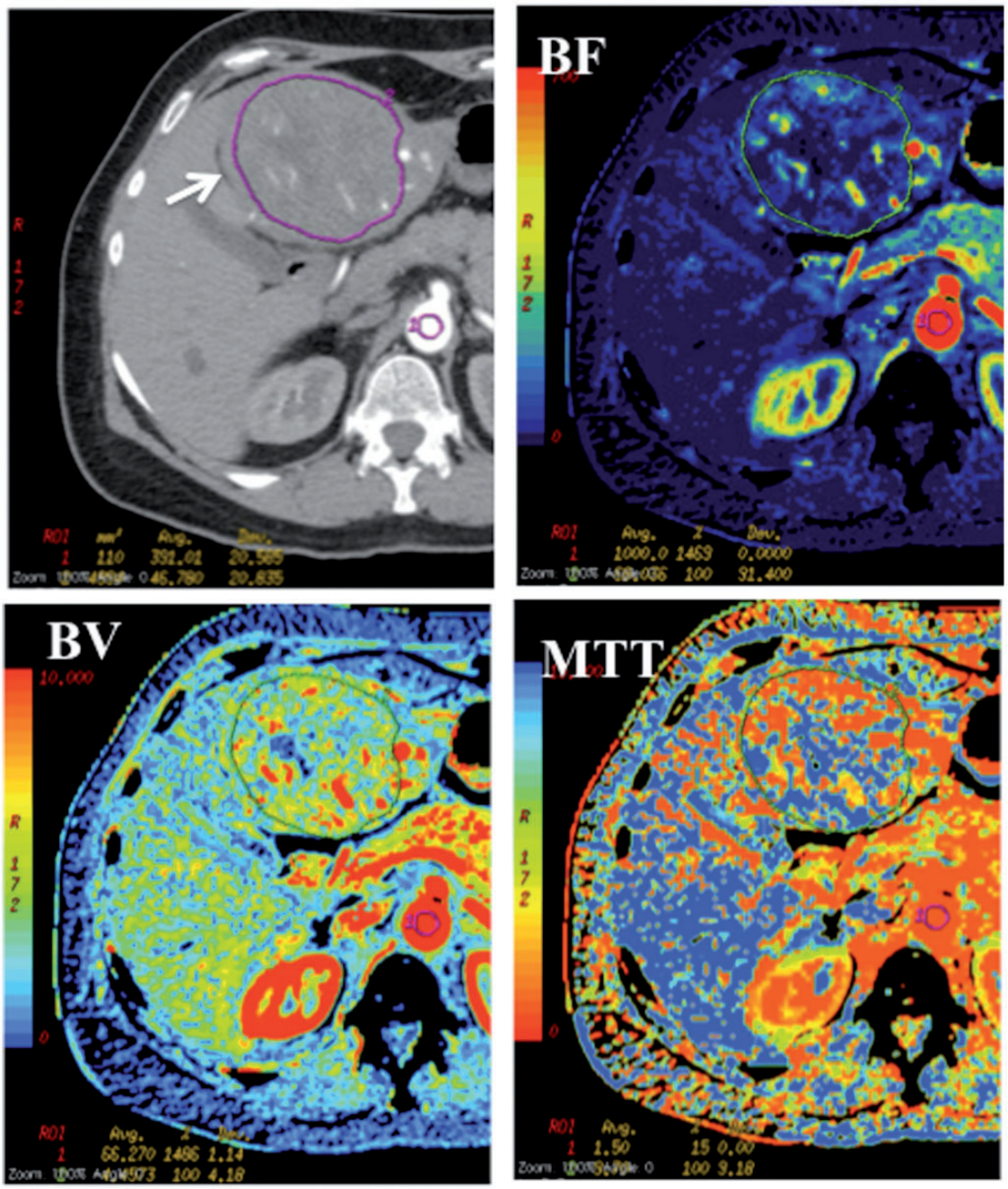

Figure 1 **Transverse CT perfusion functional map of BF, BV, and MTT in a 65-year-old woman. A region of interest was drawn freehand around the peripheral boundary of the visible tumor.**

to those of the index lesion. The established imaging features on CE-MRI and precontrast T1-weighted and T2-weighted images were applied for lesion characterization[3]. Moreover, follow-up CT and MRI examinations over a 6-month interval were available for all of the patients, which also confirmed tumor growth.

Statistical analysis

The perfusion parameters of liver tumors were compared between HCCs, hypervascular metastases, and hypovascular metastases. Statistical analysis was performed with Mann–Whitney *U* test for comparisons of the 2 data sets. Receiver-operator characteristic (ROC) analysis was performed to estimate the diagnostic values of perfusion parameters for distinction of HCCs from hypervascular metastases, and identify the parameter threshold at which HCCs were distinguished from hypervascular metastases. Statistical analyses were carried out using the StatView program (SAS Institute, Cary, NC, USA), and for all comparisons $P < 0.05$ was considered to indicate a statistically significant difference.

Results

Patient characteristics

Of the 34 patients enrolled, a total of 31 were included in the current study. Three patients were excluded because they had no measurable HCC in the liver and showed metastatic tumors outside the liver. Of the 31 patients included in this investigation, 20 had HCCs and 11 had liver metastases from the primary sites, being colon and rectal cancer ($n = 5$), ovarian cancer ($n = 1$), duodenal cancer ($n = 1$), pancreatic cancer ($n = 1$), germ cell tumor ($n = 1$), melanoma ($n = 1$), and pancreatic endocrine tumor ($n = 1$). The subjects included 16 men and 15 women, with a mean age of 60.3 (range 23–79) years. A total of 90 liver tumors (38 HCCs and 52 metastases) were evaluated, with 15 of 33 patients having multiple lesions in the liver. The mean tumor diameter of HCC at CT evaluation was 50.2 mm (range 14–163 mm), whereas that of metastasis was 32.6 mm (range 12–92 mm). Metastatic tumors were grouped into hypervascular and hypovascular metastases, based on their enhancement characteristics on the recently performed diagnostic arterial-portal venous phase CECT and CE-MRI. Of the 52 metastases, 16 were categorized as hypervascular metastases and the remaining 36 as hypovascular metastases (Fig. 2).

Perfusion measurements of HCCs, hypervascular metastases, and hypovascular metastases

Table 1 shows perfusion measurements of HCC, hypovascular metastasis, and hypervascular metastasis. The hypovascular metastases showed a significantly lower BF and BV, and higher MTT than HCC (all $P < 0.0001$). In addition, despite the avid arterial phase enhancement between HCC and hypervascular metastasis, there were clear differences in their perfusion values (Fig. 4). In HCC, BF, BV, and MTT were substantially lower than those in hypervascular metastases ($P = 0.02$, $P < 0.0001$, and $P = 0.03$, respectively).

Diagnostic value of CTP in the distinction of HCC from hypervascular metastasis

The diagnostic values of CTP parameters in distinguishing HCCs from hypervascular metastases were evaluated by ROC analysis. The areas under the ROC curves of BF, BV, and MTT were 0.70 (95% confidence interval (CI) 0.55–0.82), 0.95 (95% CI 0.87–0.98), and 0.69 (95% CI 0.54–0.81), respectively (Fig. 3). If the BV cutoff point was set at 6.9 ml/100 g, highest accuracy (88.9%) for HCC diagnosis was obtained with sensitivity of 86.8% and specificity of 93.8%.

Discussion

As tumor angiogenesis is a recognized critical step for malignant tumor growth and progression[18] and is closely related to evolution of both primary and secondary malignancies of the liver, a precise understanding of the tumor hemodynamics is essential for accurate imaging diagnosis to facilitate the appropriate treatment[13,19]. The development of unpaired arteries and the degree of sinusoidal capillarization is closely related to the development of HCC in a cirrhotic nodule[20,21]. Thus, in CECT, HCC tumor shows a typical hypervascular pattern, with clear-cut enhancement in the

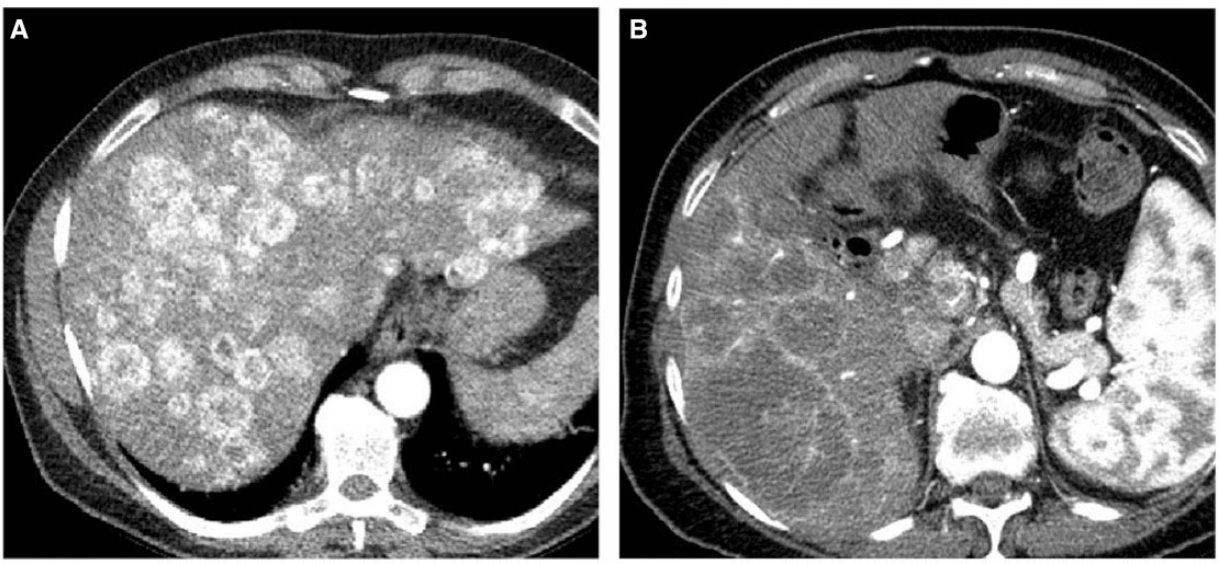

Figure 2 **Arterial phase CECT images. Metastatic liver tumors were grouped into hypervascular tumors (A) and hypovascular tumors (B).**

Table 1 **Perfusion parameters of hypovascular and hypervascular metastases compared with those of HCCs**

Perfusion parameter	HCC ($n=38$)	Hypovascular ($n=36$)	P	Hypervascular ($n=16$)	P
BF (ml/100 g/min)	112.9 ± 57.1	22.1 ± 14.7	<0.0001	143.0 ± 28.6	0.02
BV (ml/100 g)	4.8 ± 1.9	1.9 ± 0.9	<0.0001	10.1 ± 2.8	<0.0001
MTT (s)	4.8 ± 2.5	9.9 ± 5.6	<0.0001	5.9 ± 1.3	0.03

BF, blood flow; BV, blood volume; MTT, mean transit time.

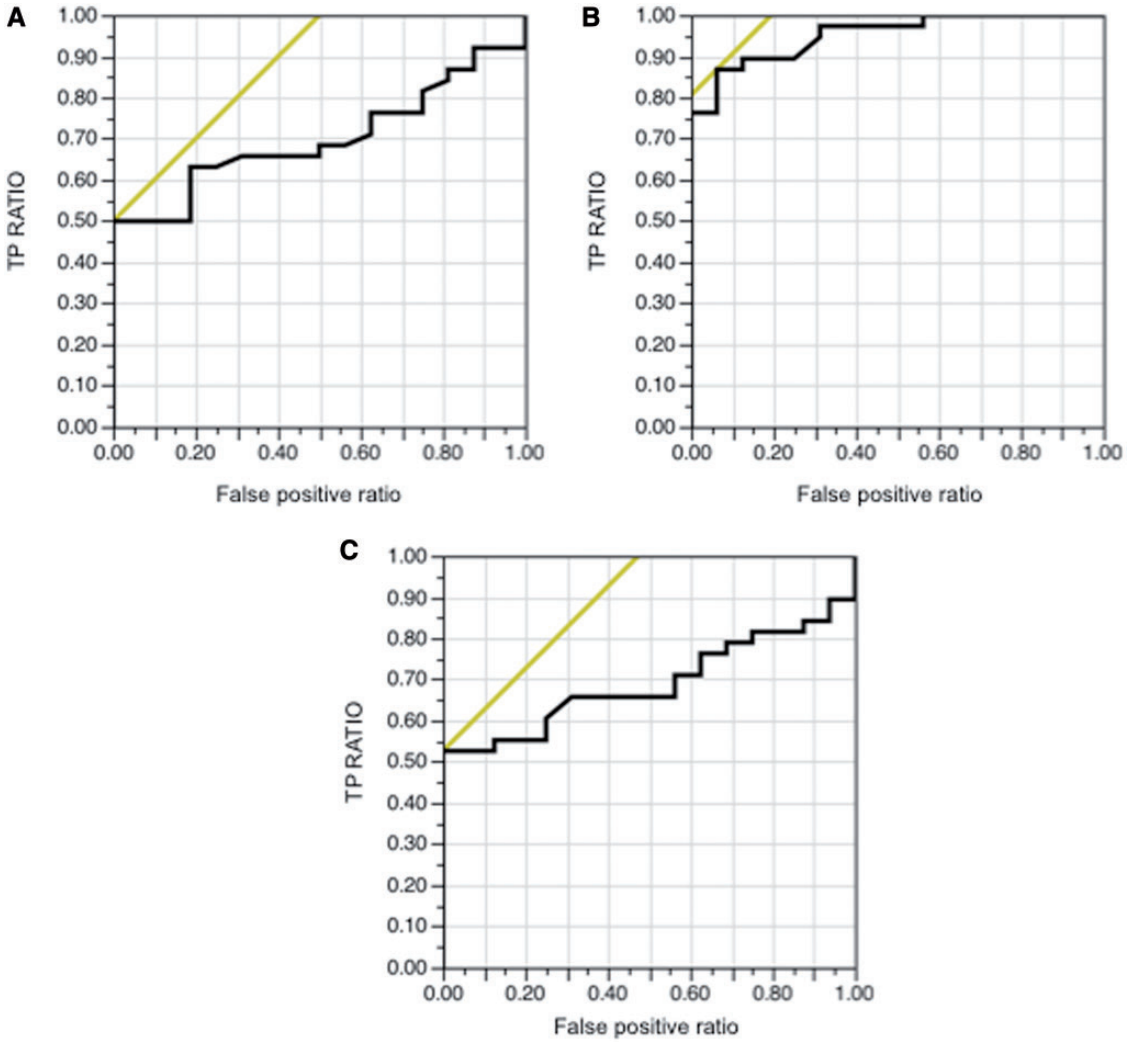

Figure 3 **The diagnostic values of CTP parameters in distinguishing HCCs from hypervascular metastases were also evaluated by ROC analysis. The areas under the ROC curves of BF, BV, and MTT were 0.70, 0.95, and 0.69, respectively.**

predominantly arterial phase and rapid washout in the portal venous phase[3]. On the other hand, metastatic liver metastases generally occur in noncirrhotic liver[22], and develop varying degrees of hepatic arterial blood supply. Liver metastases that have predominantly hepatic arterial blood supply (hypervascular) are conspicuous in the hepatic arterial dominant phase, while hypovascular metastases that are predominantly supplied by portal venous branches demonstrate slower and less intense enhancement, making them more conspicuous in portal venous phase images[23]. Thus, there is an overlap in the enhancement pattern between HCCs and hypervascular metastases[7]. In addition, 15–43% of the cases of HCC in North America occur in patients without evidence of cirrhosis[24–26]. If we encounter a patient who develops hypervascular tumors in a noncirrhotic liver,

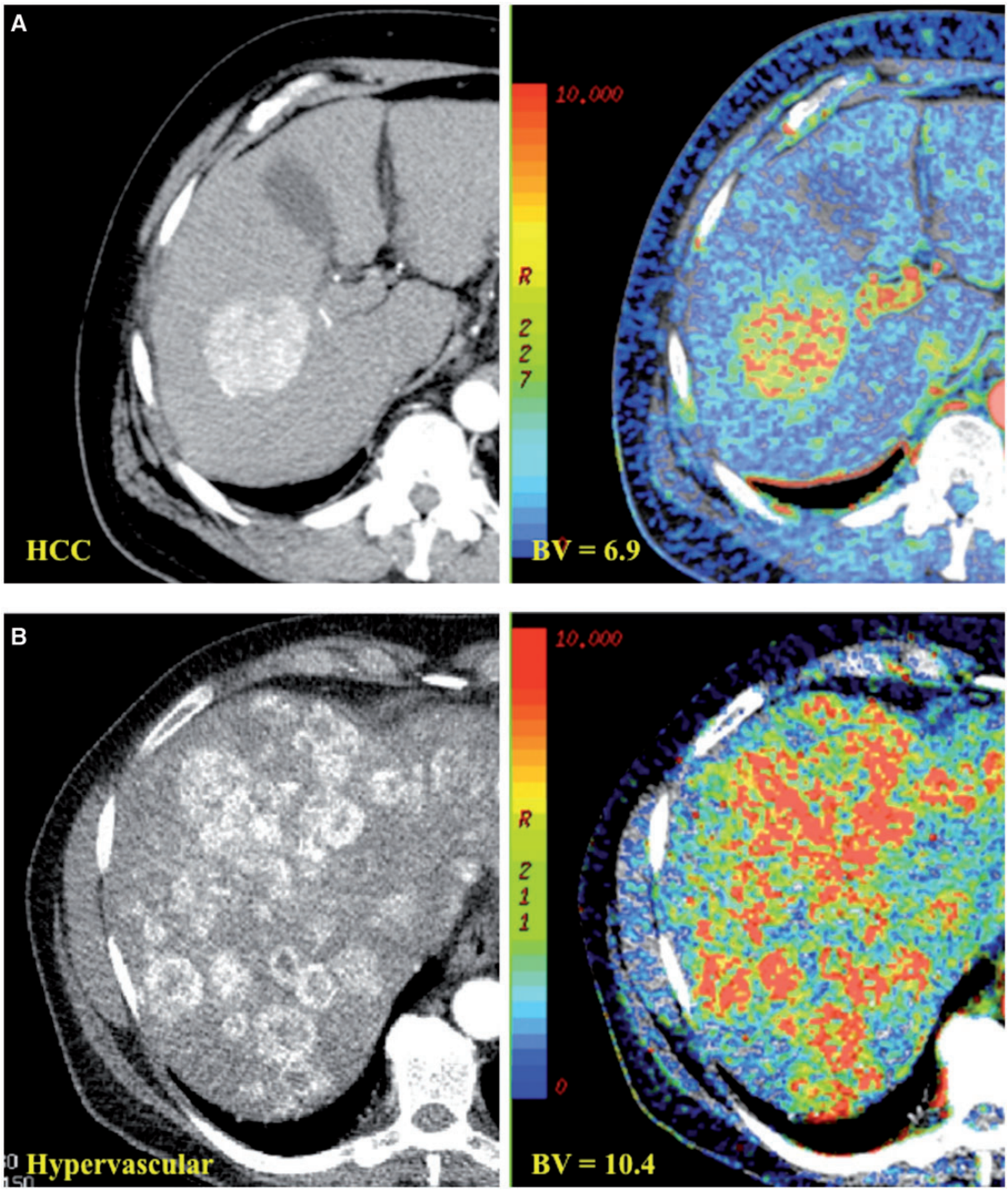

Figure 4 **Differentiation of HCC from other hypervascular metastasis in the liver is occasionally difficult. However, we observed clear differences in their BV value. (A) HCC (BV = 6.9). (B) Metastases of a pancreatic endocrine tumor (BV = 10.4).**

it might be difficult to distinguish HCC from hypervascular metastasis[4].

Dynamic imaging methods using CT or MRI, which have been shown to indirectly reflect underlying tumor biology or microvascular environment, have been expected to be a useful marker for diagnosis or evaluating early treatment response in cancer treatment[12,15,27,28]. A previous study has demonstrated that CTP is a feasible and reproducible technique for assessing tissue perfusion in HCC, with well-differentiated HCC showing higher perfusion values than other grades[12]. Jiang et al.[16] reported that CTP was a more sensitive marker for monitoring the antiangiogenic treatment effect. In MRI studies, Abdullah et al.[27] demonstrated the usefulness of dynamic MRI in characterizing liver tumors, and Hsu et al.[28] demonstrated the use of dynamic MRI to predict clinical outcome of HCC treated with an antiangiogenic agent.

In our study, HCC demonstrated substantially higher BF, BV, and lower MTT in comparison with hypovascular metastasis. These results are consistent with previous CT and MRI perfusion studies between HCC and colorectal liver metastasis[11,27]. These studies reported that HCC had higher perfusion and lower MTT than metastasis, because most metastases, especially those from adenocarcinomas of the gastrointestinal tract, usually enhance less and take up contrast material more slowly, with less enhancement represented as low perfusion values[29–31].

However, to date no study has directly compared differences in CTP values between HCCs and hypervascular metastases. In our study, HCC showed substantially lower BV than hypervascular metastasis, and ROC analysis revealed that tumor BV might be a useful marker to distinguish HCCs from hypervascular metastases. BF and MTT showed significant differences between HCCs and hypervascular metastases, but the range overlap might make it unsuitable for differentiation between them. Guyennon et al.[32] reported CTP values of liver metastases from neuroendocrine tumors. In their study, neuroendocrine liver metastasis showed a higher BV value (20.8 ml/100 g) than those of HCC in our study or previous reports (4.8–5.46 ml/100 g)[13,16]. We assume that the resistance to the drainage in HCC might explain the difference in BV between HCC and hypervascular metastasis. In HCC, the communication between tumor sinusoids and the surrounding hepatic sinusoids are blocked with pseudocapsule formation and fibrosis of surrounding liver[21]. This resistance is expected to increase microvascular resistance, therefore BV might decrease in HCC to a greater extent than in metastasis[33].

Our study has a few limitations. First, our findings are based on data from a single center, and the sample size was small. In addition, we did not study liver metastases from all potential primary sites, therefore it remains unknown whether all the metastases will display a similar perfusion profile. Second, the CTP technique is evolving, with a lack of consensus and standardization of data acquisition and analysis methods. The definition of the tumor ROI and the acquisition time is subject to similar consideration[34,35]. Third, even though the liver has both arterial and portal blood supply, CTP analysis was performed by using a single arterial input; the portal vein could not be consistently included either, because of the limited scanning range of CTP. We assume that the contribution to perfusion value estimates is minimal because perfusion scanning was performed for less than 40 s after the initiation of CM administration, but this possibility cannot be entirely excluded[13].

Conclusion

Today, CT is the most common modality for evaluating cancer patients. Our study suggests that CTP may help to differentiate HCC from metastasis in the liver, even if hypervascular metastasis mimics HCC. To obtain more conclusive results, a larger patient population should be studied. However, we hope that CTP becomes a useful marker to aid the diagnosis of liver tumors and leads to more accurate diagnosis.

Conflict of interest

The authors declare that they have no conflicts of interest.

References

[1] Okuda K. Hepatocellular carcinoma: clinicopathological aspects. J Gastroenterol Hepatol 1997; 12: 314–318.
[2] Choi BY, Nguyen MH. The diagnosis and management of benign hepatic tumors. J Clin Gastroenterol 2005; 39: 401–412.
[3] Bruix J, Sherman M. Management of hepatocellular carcinoma. Hepatology 2005; 42: 1208–1236.
[4] Choi BI, Han JK, Cho JM, et al. Characterization of focal hepatic tumors. Cancer 1995; 76: 2433–2442.
[5] Passe TJ, Bluemke DA, Siegelman SS. Tumor angiogenesis: tutorial on implications for imaging. Radiology 1997; 203: 593–600.
[6] Baron RL, Oliver 3rd JH, Dodd 3rd GD, Nalesnik M, Holbert BL, Carr B. Hepatocellular carcinoma: evaluation with biphasic, contrast-enhanced, helical CT. Radiology 1996; 199: 505–511.
[7] Bhayana D, Kim TK, Jang HJ, Burns PN, Wilson SR. Hypervascular liver masses on contrast-enhanced ultrasound: the importance of washout. AJR Am J Roentgenol 2010; 94: 977–983.
[8] Miles KA, Hayball M, Dixon AK. Colour perfusion imaging: a new application of computed tomography. Lancet 1993; 337: 643–645.
[9] Ronot M, Asselah T, Paradis V, et al. Liver fibrosis in chronic hepatitis C virus infection: differentiating minimal from intermediate fibrosis with perfusion CT. Radiology 2010; 256: 135–142.
[10] Hashimoto K, Murakami T, Dono K, et al. Assessment of the severity of liver disease and fibrotic change: the usefulness of hepatic CT perfusion imaging. Oncol Rep 2006; 16: 677–683.
[11] Van Beers BE, Leconte I, Materne R, Smith AM, Jamart J, Horsmans Y. Hepatic perfusion parameters in chronic liver disease: dynamic CT measurement correlated with disease severity. AJR Am J Roentgenol 2001; 176: 667–673.
[12] Tsushima Y, Funabasama S, Aoki J, Sanada S, Endo K. Quantitative perfusion map of malignant liver tumors, created from dynamic computed tomography data. Acad Radiol 2004; 11: 215–233.
[13] Sahani DV, Holalhere NS, Mueller PR, Zhu AX. Advanced hepatocellular carcinoma: CT perfusion of liver and tumor tissue–initial experience. Radiology 2007; 243: 736–743.
[14] Miles KA, Leggett DA, Kelley BB, Hayball MP, Sinnatamby R, Bunce I. In vivo assessment of neovascularization of liver metastases using perfusion CT. Br J Radiol 1998; 71: 276–281.
[15] Ippolito D, Capraro C, Casiraghi A, Cestari C, Sironi S. Quantitative assessment of tumour associated neovascularization in patients with liver cirrhosis and hepatocellular carcinoma: role of dynamic-CT perfusion imaging. Eur Radiol 2012; 22: 803–811.
[16] Jiang T, Kambadakone A, Kuikarni NM, Zhu AX, Sahani DV. Monitoring response to antiangiogenic treatment and predicting outcomes in advanced hepatocellular carcinoma using image biomarkers, CT perfusion, tumor density, and tumor size (RECIST). Invest Radiol 2012; 47: 11–17.

[17] Jiang HJ, Lu HB, Zhang ZR, et al. Experimental study on angiogenesis in a rabbit VX2 early liver tumour by perfusion computed tomography. J Int Med Res 2010; 38: 929–939.
[18] Hanahan D, Folkman J. Patterns and emerging mechanisms of the angiogenic switch during tumorigenesis. Cell 1996; 86: 353–364.
[19] Matsui O, Kobayashi S, Sanada J, et al. Hepatocellular nodules in liver cirrhosis: hemodynamic evaluation (angiography-assisted CT) with special reference to multi-step hepatocarcinogenesis. Abdom imaging 2011; 36: 264–272.
[20] Ueda K, Terada T, Nakanuma Y, Matsui O. Vascular supply in adenomatous hyperplasia of the liver and hepatocellular carcinoma: a morphometric study. Hum Pathol 1992; 23: 619–626.
[21] Park YN, Kim YB, Yang KM, Park C. Increased expression of vascular endothelial growth factor and angiogenesis in the early stage of multistep hepatocarcinogenesis. Arch Pathol Lab Med 2000; 124: 1061–1065.
[22] Seymour K, Charnley RM. Evidence that metastasis is less common in cirrhotic than normal liver: a systematic review of post-mortem case-control studies. Br J Surg 1999; 86: 1237–1242.
[23] Namasivayam S, Martin DR, Saini S. Imaging of metastases: MRI. Cancer Imaging 2007; 7: 2–9.
[24] Okuda K. Hepatocellular carcinoma. J Hepatol 2000; 32: 225–237.
[25] Nzeako UC, Goodman ZD, Ihsak KG. Hepatocellular carcinoma in cirrhotic and noncirrhotic livers: a clinico-histopathologic study of 804 North American patients. Anat Path 1996; 105: 67–75.
[26] Yamashita Y, Takahashi M, Baba Y, et al. Hepatocellular carcinoma with or without cirrhosis: a comparison of CT and angiographic presentation in the United States and Japan. Abdom Imaging 1995; 18: 168–175.
[27] Abdullah SS, Pialat JB, Wiart M, et al. Characterization of hepatocellular carcinoma and colorectal liver metastasis by means of perfusion MRI. J Magn Reson Imaging 2008; 28: 390–395.
[28] Hsu CY, Shen YC, Yu CW. Dynamic contrast-enhanced magnetic resonance imaging biomarkers predict survival and response in hepatocellular carcinoma patients treated with sorafenib and metronomic tegafur/uracil. J Hepatol 2011; 55: 858–865.
[29] Foley WD, Berland LL, Lawson TL, Smith DF, Thorsen MK. Contrast enhancement technique for dynamic hepatic computed tomography scanning. Radiology 1983; 147: 797–803.
[30] Sager EM, Scheel B, Talle K. Increase detectability of liver metastases by the use of contrast enhancement in computed tomography: a comparison between the precontrast, the immediate postcontrast and the one hour postcontrast scan. Acta Radiol 1985; 26: 369–372.
[31] Dean PB, Violante MR, Mahoney JA. Hepatic CT contrast enhancement: effect of dose, duration of infusion, and time elapsed following infusion. Invest Radiol 1980; 15: 158–161.
[32] Guyennon A, Mihaila M, Palma J, Lombard-Bohas C, Chayvialle JA, Pilleul F. Perfusion characterization of liver metastases from endocrine tumors: computed tomography perfusion. World J Radiol 2010; 2: 449–454.
[33] Chen ML, Zeng QY, Huo JW, Yin XM, Li BP, Liu JX. Assessment of the hepatic microvascular changes in liver cirrhosis by perfusion computed tomography. World J Gastroenterol 2009; 15: 3532–3537.
[34] Goh V, Halligan S, Hugill JA, Gartner L, Bartram CI. Quantitative colorectal cancer perfusion measurement using dynamic contrast-enhanced multidetector-row computed tomography: effect of acquisition time and implication for protocols. J Comput Assist Tomogr 2005; 29: 59–63.
[35] Ng CS, Chandler AG, Wei W, et al. Reproducibility of CT perfusion parameters in liver tumors and normal liver. Radiology 2011; 260: 762–770.